Supplement of

Sensitivity of young water fractions to hydro-climatic forcing and landscape properties across 22 Swiss catchments

Jana von Freyberg et al.

Correspondence to: Jana von Freyberg (jana.vonfreyberg@usys.ethz.ch)

- Table S1 with additional data about the phases of the seasonal precipitation regimes, as well as hydrologic soil properties and hydrogeological characteristics of the individual study sites
- Detailed description of an alternative interpolation method for precipitation isotopes (method 2)
- *R* script for performing iteratively reweighted least squares (IRLS) regression with optional point weights, including a demo data set ("*IRLS_hess-2017-720.R*")

Table S1: Elevation ranges, as well as hydrologic soil properties and hydrogeological characteristics of the 22 Swiss study catchments.

Catchment name	Phase of seasonality of monthly precipitation φ_{precip} (months)	Fraction of shallow soils (%)	Fraction of low - medium water storage capacity soils (%)	Fraction of high - very high permeability soils (%)	Fraction of aquifers with low productivity (%)	Fraction of aquifers with intermediate productivity (%)	Fraction of aquifers with high productivity (%)
Aabach	3.8	0	0	23	87	0	13
Aach	3.9	0	0	0	86	0	14
Allenbach	3.2	78	57	30	89	11	0
Alp	3.2	68	48	1	81	6	12
Biber	3.3	30	30	0	94	0	6
Dischmabach	3.5	59	59	59	92	9	0
Emme	3.3	78	49	21	88	11	0
Ergolz	4.0	42	41	28	42	54	5
Erlenbach	3.2	100	4	0	82	18	0
Guerbe	3.6	48	35	45	70	17	13
Ilfis	3.3	32	28	42	92	1	7
Langeten	3.4	0	0	37	77	13	10
Lümpenenbach	3.1	100	4	0	100	0	0
Mentue	4.7	0	0	76	99	0	0
Murg	3.7	0	0	9	87	1	12
Ova da Cluozza	3.4	34	34	34	8	92	0
Riale di Calneggia	3.3	39	44	44	96	4	0
Rietholzbach	3.7	0	0	0	100	0	0
Schaechen	3.5	73	67	23	76	24	0
Sense	3.6	39	24	47	85	10	5
Sitter	3.2	71	61	36	48	52	0
Vogelbach	3.2	100	51	0	100	0	0

An alternative interpolation method for precipitation isotopes (method 2)

Method 2 for the spatial interpolation of precipitation isotopes is based on the approach developed by Allen et al. (2018), and is briefly described here. Precipitation $\delta^{18}O$ measurements from 19 long-term monitoring stations in Switzerland (13 stations from NAQUA-ISOT, the Swiss network for Observations of Isotopes in the Water Cycle) and Germany (6 stations from GNIP, the Global Network of Isotopes in Precipitation) were decomposed into sine functions and time series of residuals from the sine functions.

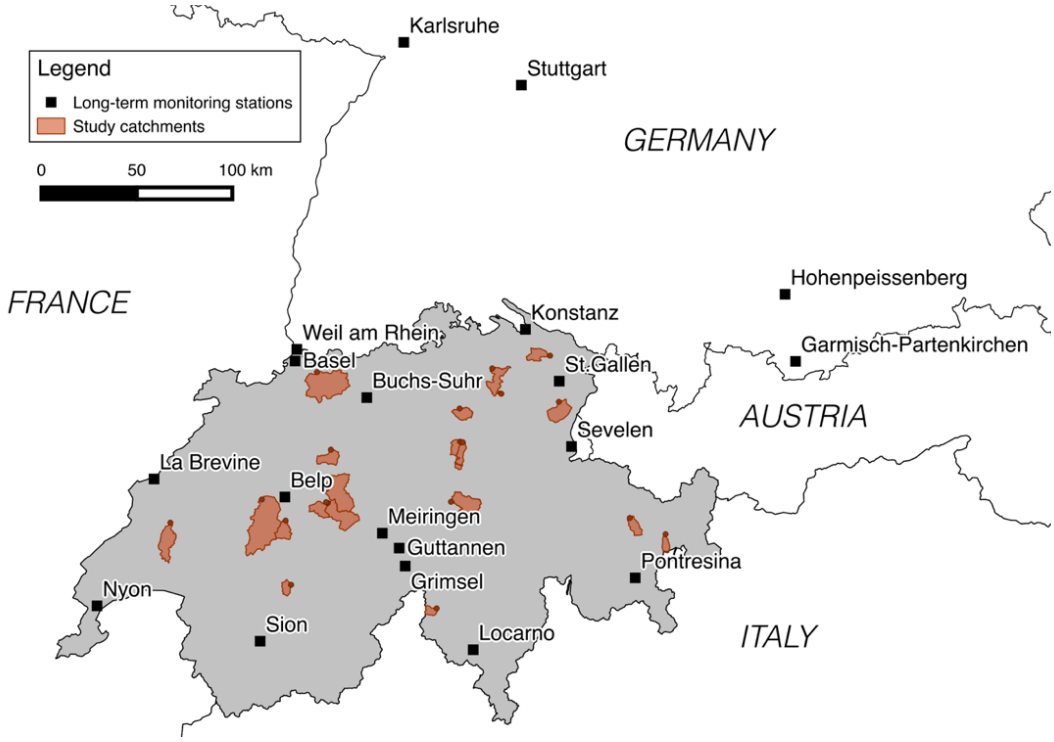

Figure S 1: Locations of the 19 long-term monitoring stations for precipitation isotopes in Germany and Switzerland used for method 2, as well as the locations of the 22 study catchments in Switzerland (see Fig. 1 and Sect. 3 in the main text for a detailed description of the study catchments).

The precipitation $\delta^{18}O$ measurements *c(t)* were fitted to sine curves through least squares regression:

$$c(t) = A\sin(2\pi ft - \varphi) + k \quad \text{(S1)}$$

In Eq. (S1), A is the amplitude (‰), φ is the phase of the seasonal cycle (rad, with 2π rad equalling 1 year), t is the time (decimal years), f is the frequency (1 year^{-1}) and k (‰) is a constant describing the vertical offset of the isotope signal. The mean RMSE for the sine fits across all measurement stations was 2.1 ‰ $\delta^{18}O$.

Each of the three parameters describing the best-fit sine functions (A, φ, and k) of the 19 long-term monitoring stations were interpolated for all of Switzerland using multiple linear regression models based on latitudes, longitudes, and elevations:

$$A = 0.0002 \cdot \text{elevation} + 0.22 \cdot \text{longitude} - 0.88 \cdot \text{latitude} + 3.97 \quad , \quad \text{(S2)}$$

$$\varphi = -3.47 \cdot 10^{-5} \cdot \text{elevation} + 0.007 \cdot \text{longitude} + 0.049 \cdot \text{latitude} - 1.82 \quad , \tag{S3}$$

$$k = -0.0025 \cdot \text{elevation} - 0.38 \cdot \text{longitude} + 0.50 \cdot \text{latitude} - 10.4 \quad . \tag{S4}$$

The explanatory variables in Eqs. (S2) - (S4) have been centered around their means, so that the intercepts describe the average latitudes, longitudes and elevations of the 19 stations, rather than an extrapolation to the arbitrary values latitude=0, longitude=0, and elevation=0.

The performance of the multiple-regression models that describe the spatial variations of the best-fit sine functions was quantified by RMSE, R^2 and the p-values of the individual coefficients (Table S2):

Table S2: RMSE, R^2 and the p-values of the individual coefficients of the multiple-regression models.

	RMSE	R^2	Elevation (p value)	Longitude (p value)	Latitude (p value)	Intercept (p value)
Amplitude A	0.70‰	0.56	0.62	0.16	0.004	$1.6 \cdot 10^{-13}$
Phase of the seasonal cycle φ	0.09rad	0.29	0.51	0.72	0.15	$5.8 \cdot 10^{-22}$
Constant k	0.66‰	0.87	0.00001	0.01	0.06	$3.25 \cdot 10^{-20}$

It should be noted that the three station properties were not strongly correlated with one another (i.e., R=0.23 and p=0.35 for elevation versus longitude; R=-0.42 and p=0.07 for elevation versus latitude; R=0.30 and p=0.21 longitude versus latitude). The linear regression models were used to model sine parameters (A, φ, and k) for every 200m pixel in the 22 Swiss study catchments.

In a second step, the time series of residuals from the sine functions were geostatistically interpolated for every month of the time period 2010-2015 and every 200m pixel in the 22 Swiss study catchments. The spatial interpolation was carried out through ordinary kriging, applying an exponential variogram model. Monthly maps of residuals from the sine functions were then used to adjust the base sinusoidal pattern for each 200m pixel in the 22 Swiss study catchments.

To quantify the prediction error of this interpolation method, it was run iteratively to simulate the monthly precipitation isotopic composition for each of the 19 long-term monitoring stations. For each of the 19 iterations, the precipitation isotope time series was predicted for one station by using only the remaining 18 stations for calibration (i.e., a leave-one-out process). This two-step approach resulted in a 1.3 ‰ $\delta^{18}O$ mean absolute deviation between observations and model outputs (Figure S2).

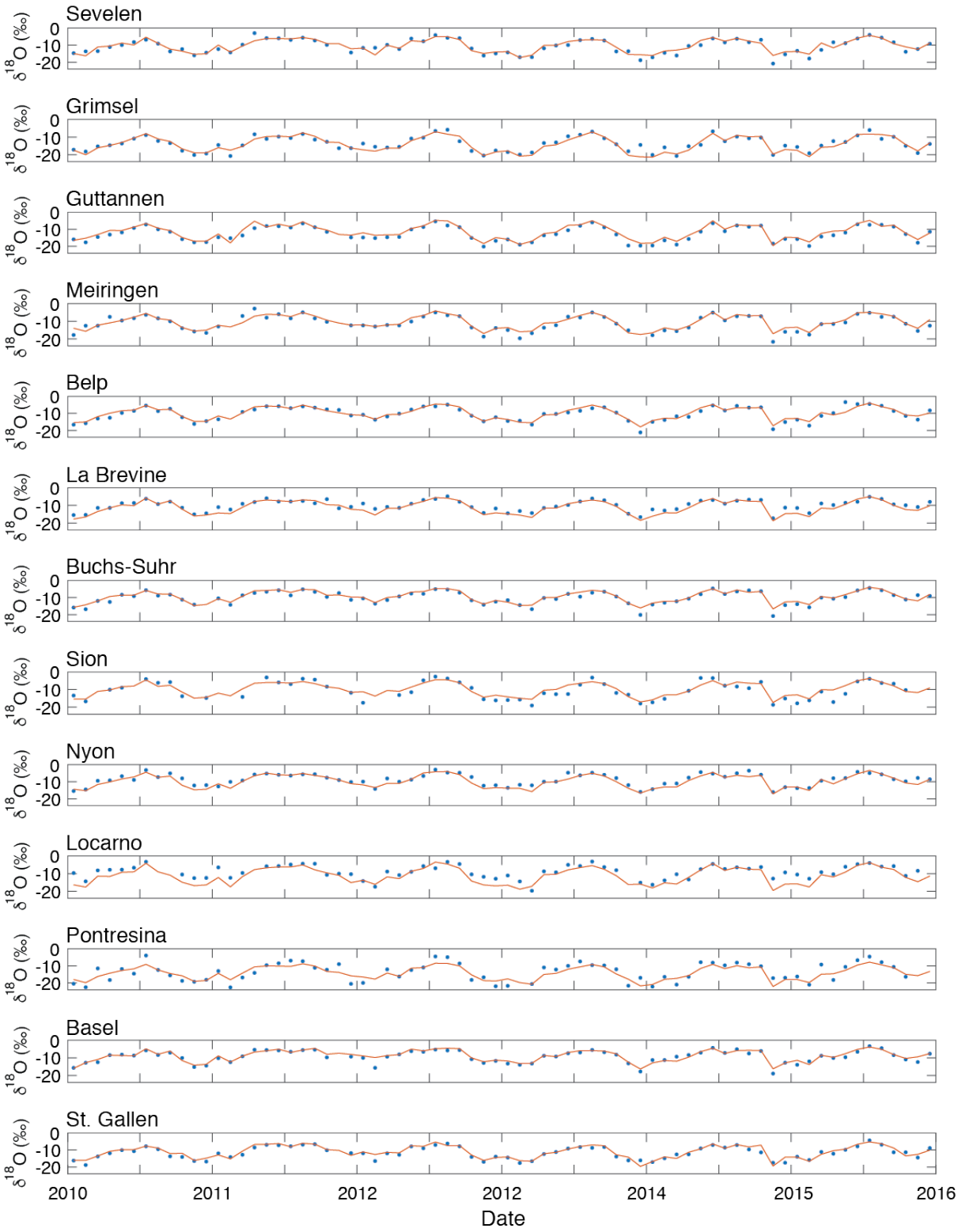

Figure S2: Modelled monthly isotope ($\delta^{18}O$) time series predicted for the 13 Swiss long-term monitoring stations (Figure S 1). The precipitation isotope time series were predicted for one station at a time by using only the remaining 18 stations (i.e., the other 12 Swiss stations and 6 German stations) for calibration (i.e., a leave-one-out process). Dots indicate the monthly observations, while lines indicate the modelled time series.

Similar to interpolation method 1 (Seeger and Weiler, 2014), monthly isotope values obtained with method 2 were volume-weighted for each pixel based on the monthly elevation-dependent precipitation volumes obtained from the PREVAH model (Viviroli et al., 2009). Next, the monthly precipitation isotope values were aggregated across all 200m pixels in each catchment for a volume-weighted, catchment-averaged precipitation isotope time series. Snow accumulation and melt were not distinguished from liquid precipitation; that is to say, precipitation was treated as a direct input to the catchment at time of falling and snowpack storage was considered to be part of catchment storage (see Sect. 4.2 in main text).

The mass-weighted, catchment-averaged precipitation isotope time series were used for obtaining the parameter A_P (Eqs. (1), (3), and (5) in the main text). For the 22 study catchments, the approach presented above resulted in different A_P values than those obtained by method 1 (Seeger and Weiler, 2014), which predicted higher A_P values for higher elevation sites (Fig. 3 in the main text). In applying the alternative method described here, we find that elevation is a weak predictor of seasonal cycle amplitudes A (Table S2). In contrast to method 1, we find that A was primarily controlled by latitude and longitude, resulting in the largest A_P values for catchments in south-eastern Switzerland (Dischmabach and Ova da Cluozza). However, spatial variations in $\delta^{18}O$ in precipitation are not simply a product of elevation (as in method 1) or of elevation, latitude, and longitude (method 2), because both methods presented here used kriging to incorporate other possible isotope effects.

Table S 3: Long-term monitoring stations with their latitudes, longitudes and elevations used for the interpolation method presented here.

Long-term monitoring station	Latitude	Longitude	Elevation (m a.s.l.)
Sevelen (CH)	47.12	9.49	457
Grimsel (CH)	46.57	8.33	1950
Guttannen (CH)	46.66	8.29	1055
Meiringen (CH)	46.73	8.18	632
Belp (CH)	46.90	7.51	515
La Brevine (CH)	46.98	6.61	1042
Buchs-Suhr (CH)	47.37	8.08	397
Sion (CH)	46.22	7.34	482
Nyon (CH)	46.38	6.23	436
Locarno (CH)	46.17	8.79	379
Pontresina (CH)	46.49	9.90	1742
Basel (CH)	47.54	7.58	319
St.Gallen (CH)	47.43	9.42	805
Konstanz (GER)	47.68	9.19	443
Weil am Rhein (GER)	47.60	7.59	249
Karlsruhe (GER)	49.04	8.37	112
Hohenpeissenberg (GER)	47.80	11.01	977
Stuttgart (GER)	48.83	9.20	314
Garmisch-Partenkirchen (GER)	47.48	11.06	719

References

Allen, S. T., Kirchner, J. W., and Goldsmith, G. R.: Predicting Spatial Patterns in Precipitation Isotope (δ2H and δ18O) Seasonality Using Sinusoidal Isoscapes, Geophysical Research Letters, doi:10.1029/2018GL077458, 2018.

Seeger, S., and Weiler, M.: Reevaluation of transit time distributions, mean transit times and their relation to catchment topography, Hydrol. Earth Syst. Sci., 18, 4751-4771, 2014.

Viviroli, D., Zappa, M., Gurtz, J., and Weingartner, R.: An introduction to the hydrological modelling system PREVAH and its pre- and post-processing-tools, Einvironmental Modelling & Software, 24, 1209-1222, 10.1016/j.envsoft.2009.04.001, 2009.